



## Determination the density of cometary nucleus material using gamma ray attenuation

Aseel A. Temur\*, Alaa B. Kadhim

Department of Astronomy and Space, College of Science, University of Baghdad, Baghdad, Iraq

### Abstract

In this work, the technique of attenuation of gamma ray to calculate the density of comet nucleus materials (C/2009 P1 (GARRADD) at different range of energy (0.2- 0.9 MeV). also, the single scattering model for gamma rays has been assumed that photons reaching the detector with scattered only once in the material. The program has been designed and written in FORTRAN language (77 – 90) to calculate the density for molecules using Monte Carlo method was used to simulate the scattering and absorption of photons in semi- infinite material. Gamma ray interacts with the matter by three mainly interactions: Photoelectric effect, Compton scattering and Pair production (electron and positron). On the  $^{137}\text{Cs}$  source energy (662 keV), Compton scattering is the dominant interaction. at energies below about 150 keV the Photoelectric effect is significant , While Pair production occurs at energies above twice the electron rest mass energy (1.022 MeV). Both these processes have mass attenuation coefficients that are heavily dependent on elemental composition, which is why only those source energies within the "Compton window" are useful for densitometry. The calculation of our results of the density were compared with the real density and the comparison is very good.

**Keywords:** Comet, density, Mass attenuation coefficient, Compton scattering, Monte Carlo Simulation, Single scattering Model.

### تحديد كثافة مواد نواة المذنب باستخدام توهين أشعة كاما

اسيل عبد تمر\*، علاء باقر كاظم

<sup>2</sup>قسم الفلك والفضاء، كلية العلوم، جامعة بغداد، بغداد، العراق

### الخلاصة

في هذا البحث تم استخدام تقنية جديدة باستخدام توهين اشعة كاما في حساب الكثافة لمواد المذنب عند مختلف الطاقات (0.2 – 0.9 MeV). ايضاً، استخدم نموذج الاستطارة المنفردة لأشعة كاما المنعكسة التي تفترض بأن الفوتونات التي تصل للكاشف تستطار مرة واحدة في المادة. استخدمت طريقة مونت كارلو لمحاكاة استطارة وامتصاص الفوتونات في المواد الشبه لا نهائية حيث تم كتابة برنامج بلغة الفورتران (77-90) لحساب كثافة الجزيئات. أشعة كاما تتفاعل مع المادة بواسطة ثلاث تفاعلات رئيسية: ظاهرة التأثير الكهروضوئي، استطارة كومبتن و انتاج الزوج (الالكترون والبوزترون). مصدر السيزيوم عند طاقة 662 keV، تحدث استطارة كومبتن، عند طاقة اقل من 150 keV تحدث ظاهرة التأثير الكهروضوئي، بينما انتاج الزوج تحدث عند طاقة تفوق الكتلة السكونية مرتان (1.022 MeV) كلا الظاهرتين معامل التوهين الكتلي يعتمد على تركيب العناصر، لذلك فإن ظاهرة كومبتن مفيدة للقياس. نتائج الكثافة المحسوبة نظرياً مقارنة بالكثافة الحقيقية جيدة جداً.

\*Email: aseeltmur869@yahoo.com

## 1. Introduction:

The comet is an important piece of the great puzzle of the solar system. It is a sort of missing link in our understanding of what created the planetary system of which the Earth is part. Basically a comet has three components that must be studied: (1) the nucleus, or center condensation, (2) the head, or coma, and (3) the tail. The nucleus is often, but not always, seen. It is the principal supply of the material from which the comet originates and is the orbiting body that encircles the Sun. Emanating from the nucleus is the coma [1]. The coma is the dusty, fuzzy cloud around the nucleus of a comet, and the tail extends from the comet and points away from the Sun. The coma and tails of a comet are transient features, present only when the comet is near the Sun [2]. Today we know that comets shine by reflected light. Their tails are formed by solar radiation pressure acting on cometary dust and molecules and by the solar wind acting on cometary ions [3].

Comets are considered among the most primitive bodies of our Solar System. In 1949 Fred Whipple hypothesized a model to describe the nature of comets (Whipple, 1949): this model became famous under the name of the “dirty snow ball” hypothesis. According to Whipple, a comet was a solid nucleus only a few kilometers in diameter, composed mainly of water ice mixed with solid particles. When far from the Sun, the nucleus is too small to be observed as resolved but, as soon as it approaches the Sun, the ices present on the top surface layers of the nucleus are released and the comet transforms in the spectacular object that people can see [4]. There are two types of comets – long and short period. Short period have orbital periods of less than 200 years while long period comets have orbital periods of more than 200 years.

**Long-period comets:** comets have very long periods of revolution that range from greater than 200 years to infinity. In other words, some long-period comets make only one pass around the Sun and do not return. Several long-period comets were discovered during the second half of the twentieth century including Hyakutake and Hale-Bopp. Both of which were seen by many people and were described in detail by Burnham (2000) [5].

**Short period comets:** comets likewise divide naturally into two groups, the Jupiter-family comets and the Halley-types. As the name suggests, a Jupiter-family comet has its destiny controlled by Jupiter [6]. Jupiter-family comets include a number of well-known comets, such as 2P/Encke, 9P/Tempel 1, 10P/Tempel 2, 19P/Borrelly, 21P/Giacobini-Zinner, 46/Wirtanen, 67P/Churyumov-Gerasimenko, 81P/Wild 2, and 103P/Hartley. Often, they originate in the Kuiper belt and exhibit orbital periods of less than 20 years. In contrast, Halley-type comets have orbital periods  $P$  that range between 20 and 200 years. The Halley family is a relatively small group, with approximately a dozen known members [7]. The best known of the short – period comets is Comet Halley, which returns every 76 years. Halley's comet was last seen in 1986 and is due to return in 2061 [8].

## 2. Monte Carlo Simulation

In this research, the Configuration of typical point isotropic source - cylindrical detector and sample were described in terms of parameters as shown in Figure-1.

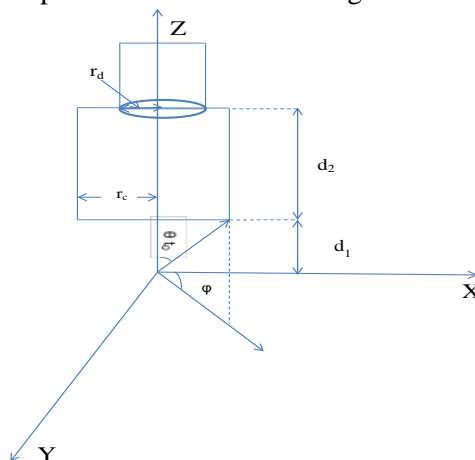


**Figure 1-** Configuration of point source and detector and sample where  $\theta$  is polar angle,  $\phi$  azimuthal angle,  $r_d$  detector radius,  $r_c$  sample material radius,  $d_1$  distance between point source and sample and  $d_2$  distance between sample and detector.

For a point source, the  $\gamma$  – photon emission direction  $\theta$  towards the front surface of the sample is calculated by

$$\theta = \cos^{-1}(2R_1 - 1) \quad (1)$$

Where R is a uniform random number ( i.e  $0 \leq R \leq 1$  ). and the azimuthal angle is sampled by the equation

$$\varphi = 2\pi R_2 \quad (2)$$

For each emitted photon.

The Coordinates of the emitted point (  $x_0, y_0$  ) is given by:

$$x_0 = R_3 \cdot A - \frac{A}{2} \quad (3)$$

$$y_0 = R_4 \cdot B - \frac{B}{2} \quad (4)$$

As seen from Figure-1. It is assumed that photons do not interact in the distance ( $t_0 = \frac{d_1}{\cos \theta}$ ) between the source and the sample until they reach the sample, and that their directions do not change the Coordinates of the point where the photon hit the plane of the front surface of the compound are.

$$X_1 = t_0 \sin \theta \cos \varphi \quad (5)$$

$$Y_1 = t_0 \sin \theta \sin \varphi \quad (6)$$

$$Z_1 = d_1 \quad (7)$$

It was controlled by the expression:

$$X_1^2 + Y_1^2 \leq r_c^2 \quad (8)$$

Whether this point was on the front surface of the material.

If the condition was unsatisfied, the photon did not enter the front surface of the material and was rejected, Then the procedure with equations from 1 to 8 was repeated with a new four of uniform random numbers. If the condition was satisfied, then this point was taken as the entrance point to the material. The photon entering the material through this point travels a certain free path. By generating a new R- value this free path was given by:

$$t = \frac{1}{\mu} \ln(1 - R) \quad (9)$$

where  $\mu$  is linear attenuation coefficient of the photon for compound material. Since

$$\left(\frac{\mu}{\rho}\right)_{\text{Compound}} = \sum_i W_i \frac{\mu_i}{\rho_i}$$

Where:

$W_i$  : weight fraction of element

$\mu_i$  : linear attenuation coefficient of  $i^{\text{th}}$  element [9].

At the end of this free path, the Photon undergoes interaction, and the Coordinates of this interaction is defines as:

$$X_2 = X_1 + T_1 \cdot \sin \theta \cos \varphi$$

$$Y_2 = Y_1 + T_1 \cdot \sin \theta \sin \varphi$$

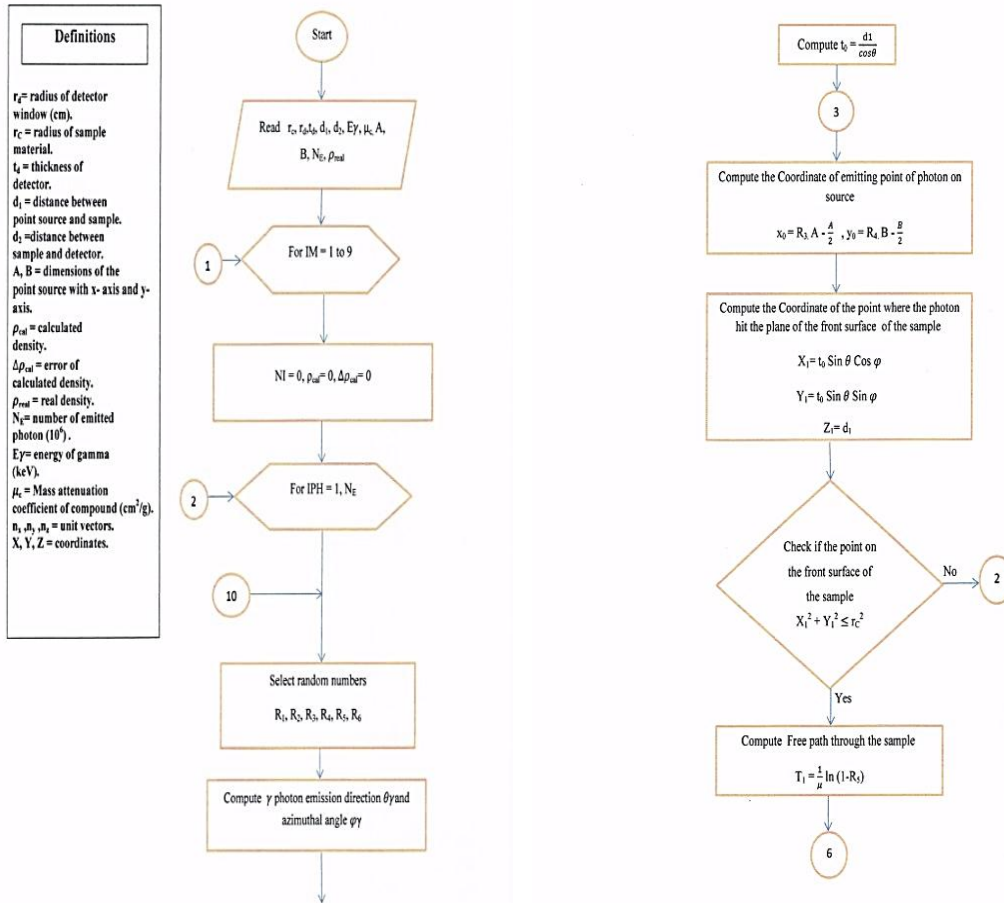
$$Z_2 = Z_1 + T \cdot \cos \theta$$

It was controlled the expression:  $X_1^2 + Y_1^2 \leq r_c^2$

### 3. Geometry of Single Scattering Models:

The use of gamma rays is an attractive solution for the measurement of bulk density on planetary surfaces. The technique relies on the Compton scattering of photons (emitted from a gamma source, usually  $^{137}\text{Cs}$ ) by electrons in the material under investigation. For a given photon energy (662 keV in the case of  $^{137}\text{Cs}$ ), the interaction cross-section for Compton scattering depends only on the number density of electrons in the material. Since the ratio of mass number to atomic number is constant

(approximately 2) for most chemical elements, the mass attenuation coefficient for photons is almost independent of composition in the region where Compton scattering is the dominant interaction. Measurements of the attenuation or scattering of gamma rays by the Compton process are thus closely related to the bulk density of the material. At energies below about 200 keV photoelectric absorption becomes significant, while at energies above about 1.5 MeV e-/e+ pair production becomes significant. Both processes have mass attenuation coefficients that are heavily composition dependent, so they are not useful for density measurements of materials of unknown composition.



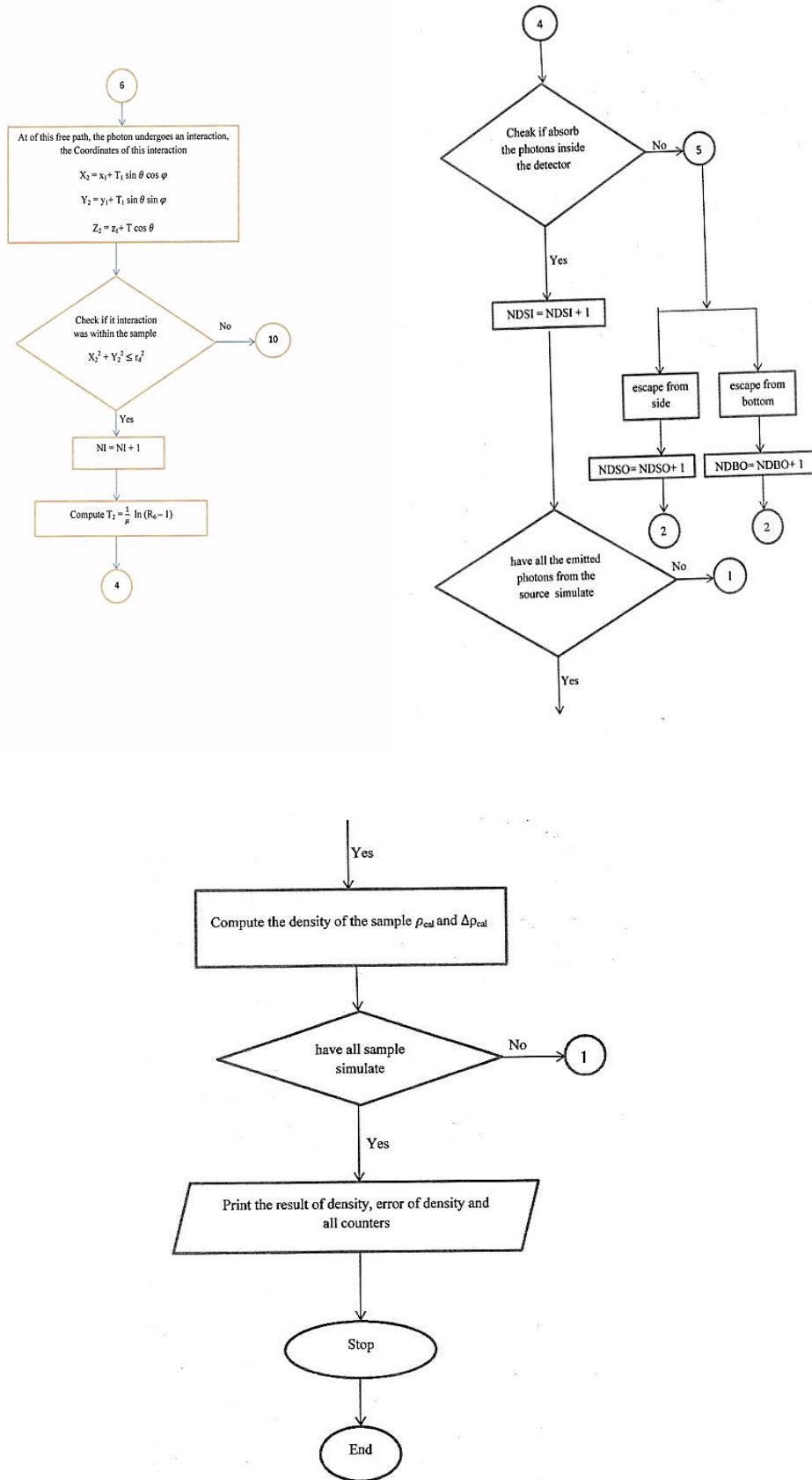


Figure 2- Flowchart for successive stages of program for simulation of photon history.

#### 4. Results and Discussion

1. The densities values of the nine molecules for C/2009 P1Garrad Comet were calculated for point source  $^{137}\text{Cs}$  - cylindrical sample- detector System and by using Monte Carlo method. This msimulation results comprised the several of runs with photon numbers  $10^6$ . The simulations involved photon energies ranging from 0.2 to 0.9 MeV including 0.662 MeV and thickness of the sample ranging from (11-20) cm in order to improve the calculations of the densities.
  2. The calculations were valid for photons at energy 0.662 MeV because the calculation depends on compton scattering interaction. The simulation program did not take into consideration the photoelectric effect and pair production.
  3. The densities values depended on the geometries of the system and the distance between the detector and source. Consequently the values varied with the detector radius and the photon energy.
  4. The calculated results are given in Figure-3 to -11, as seen clearly the number of detected photon decreases with increasing distances and increases with radius of the detector ( $R_d$ ).
5. The densities values calculated from the Monte Carlo simulation method are in good agreement with the real densities as shown in Table -10.

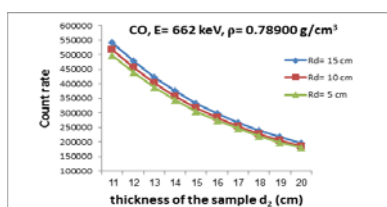


Figure 3- The variation of No. of incident photon on detector as a function of the sample thickness for CO molecule.

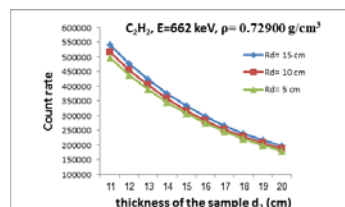


Figure 4- The variation of No. of incident photon on detector as a function of the sample thickness for  $\text{C}_2\text{H}_2$  molecule.

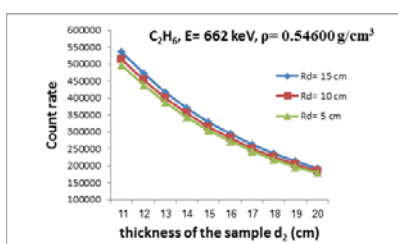


Figure 5- The variation of No. of incident photon on detector as a function of the sample thickness for  $\text{C}_2\text{H}_6$  molecule

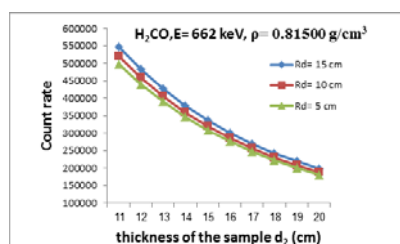


Figure 6- The variation of No. of incident photon on detector as a function of the sample thickness for  $\text{H}_2\text{CO}$  molecule.

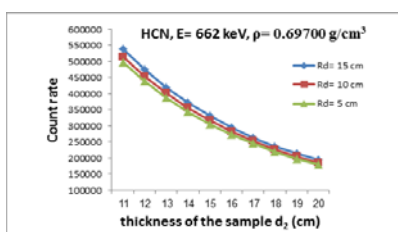


Figure 7- The variation of No. of incident photon on detector as a function of the sample thickness for HCN molecule.

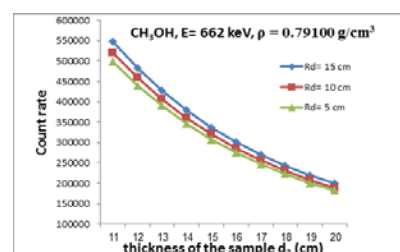


Figure 8- The variation of No. of incident photon on detector as a function of the sample thickness for  $\text{CH}_3\text{OH}$  molecule.

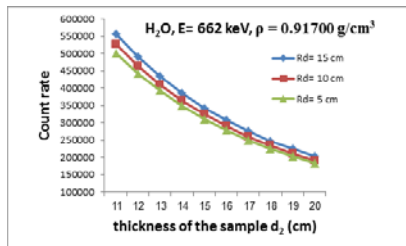


Figure 9- The variation of No. of incident photon on detector as a function of the sample thickness for H<sub>2</sub>O molecule.

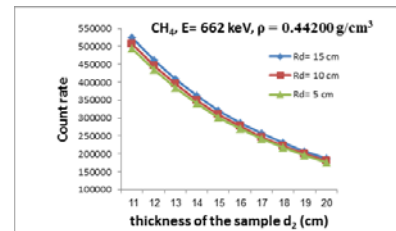


Figure 10- The variation of No. of incident photon on detector as a function of the sample thickness for CH<sub>4</sub> molecule.

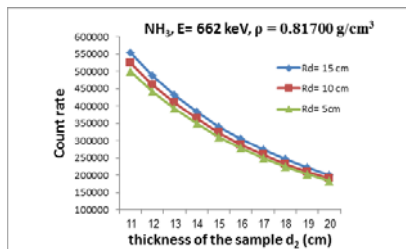


Figure 11- The variation of No. of incident photon on detector as a function of the sample thickness for NH<sub>3</sub> molecule.

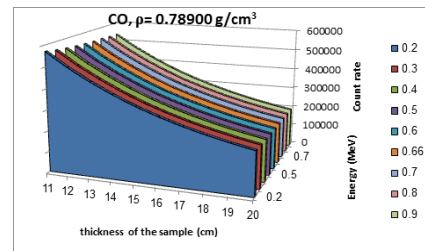


Figure 12- The variation of No. of incident photon on detector as a function of the sample thickness and photon energy for CO molecule.

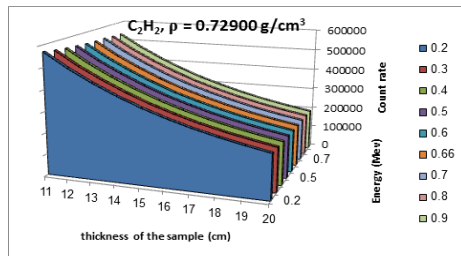


Figure 13- The variation of No. of incident photon on detector as a function of the sample thickness and photon energy for C<sub>2</sub>H<sub>2</sub> molecule.

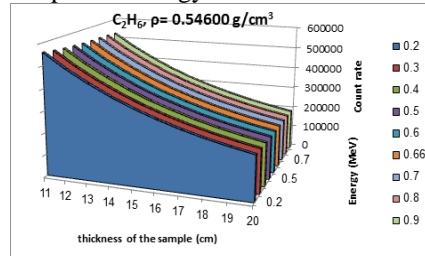


Figure 14- The variation of No. of incident photon on detector as a function of the sample thickness and photon energy for C<sub>2</sub>H<sub>6</sub> molecule.

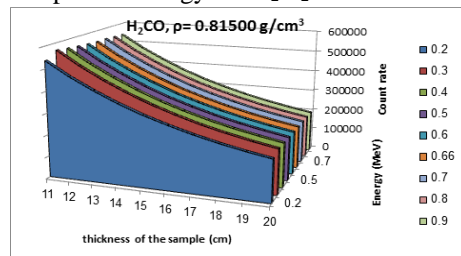


Figure 15- The variation of No. of incident photon on detector as a function of the sample thickness and photon energy for H<sub>2</sub>CO molecule.

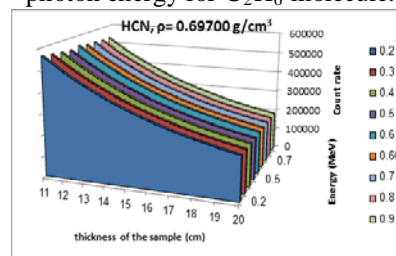


Figure 16- The variation of No. of incident photon on detector as a function of the sample thickness and photon energy for HCN molecule.

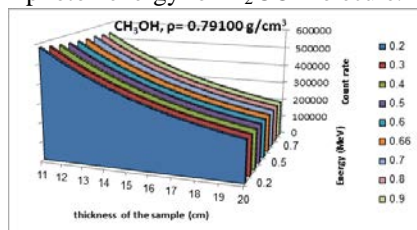


Figure 17- The variation of No. of incident photon on detector as a function of the sample thickness and photon energy for CH<sub>3</sub>OH molecule.

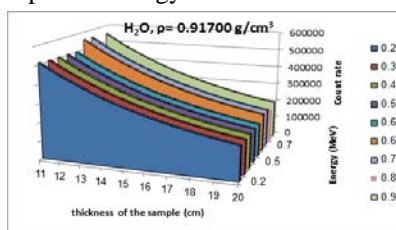
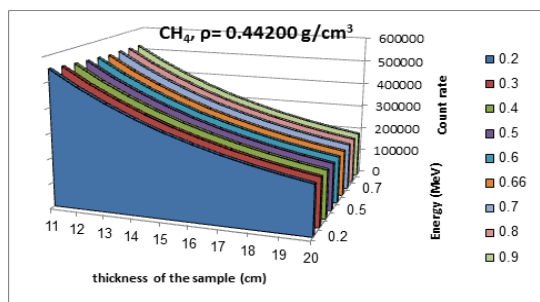
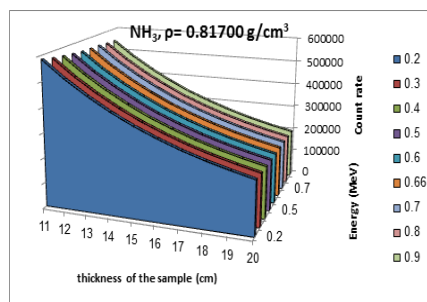


Figure 18- The variation of No. of incident photon on detector as a function of the sample thickness and photon energy for H<sub>2</sub>O molecule.



**Figure 19-** The variation of No. of incident photon on detector as a function of the sample thickness and photon energy for CH<sub>4</sub> molecule.



**Figure 20-** The variation of No. of incident photon on detector as a function of the sample thickness and photon energy for NH<sub>3</sub> molecule.

**C/2009 P1Garradd Comet**

Sample. CO

Mass attenuation coefficient = 0.07554 cm<sup>2</sup>/g

Abundance = 9.1% [10]

No. of photon = 10<sup>6</sup>

E<sub>γ</sub> = 0.662 MeV

Detector radius = R<sub>d</sub> = 15 cm

**Table 1-** Shows the calculated density for CO molecule in C/2009 P1Garradd Comet.

d <sub>1</sub> (cm)	d <sub>2</sub> (cm)	Real density (g/cm <sup>3</sup> )	Calculated density (g/cm <sup>3</sup> )	No.of incident photon on detector	Error in density (g/cm <sup>3</sup> )
5	11	0.78900	0.83979	497672	0.00209
=	12	=	0.90704	439458	0.00200
=	13	=	0.96060	389330	0.00192
=	14	=	1.00543	345312	0.00187
=	15	=	1.04318	306658	0.00182
=	16	=	1.06876	274792	0.00178
=	17	=	1.09188	246062	0.00175
=	18	=	1.10996	221080	0.00173
=	19	=	1.12331	199440	0.00171
=	20	=	1.13162	180930	0.00169

Sample. C<sub>2</sub>H<sub>2</sub>

Mass attenuation coefficient = 0.08139 cm<sup>2</sup>/g

Abundance = 0.06% [10]

No. of photon = 10<sup>6</sup>

E<sub>γ</sub> = 0.662 MeV

Detector radius = R<sub>d</sub> = 15 cm

**Table 2-** Shows the calculated density for C<sub>2</sub>H<sub>2</sub> molecule in C/2009 P1Garradd Comet.

d <sub>1</sub> (cm)	d <sub>2</sub> (cm)	Real density (g/cm <sup>3</sup> )	Calculated density (g/cm <sup>3</sup> )	No.of incident photon on detector	Error in density (g/cm <sup>3</sup> )
5	11	0.72900	0.77953	497626	0.00194
=	12	=	0.84188	439444	0.00185
=	13	=	0.89166	389288	0.00179
=	14	=	0.93335	345240	0.00173
=	15	=	0.96840	306582	0.00169
=	16	=	0.99209	274736	0.00165
=	17	=	1.01356	246008	0.00163
=	18	=	1.03044	220996	0.00160
=	19	=	1.04276	199382	0.00159
=	20	=	1.05041	180892	0.00157



Sample. C<sub>2</sub>H<sub>6</sub>

Mass attenuation coefficient = 0.09223 cm<sup>2</sup>/g

Abundance = 0.64% [10]

No. of photon = 10<sup>6</sup>

E<sub>γ</sub> = 0.662 MeV

Detector radius = R<sub>d</sub> = 15 cm

**Table 3-** Shows the calculated density for C<sub>2</sub>H<sub>6</sub> molecule in C/2009 P1 Garrard Comet.

d <sub>1</sub> (cm)	d <sub>2</sub> (cm)	Real density (g/cm <sup>3</sup> )	Calculated density (g/cm <sup>3</sup> )	No.of incident photon on detector	Error in density (g/cm <sup>3</sup> )
5	11	0.54600	0.69138	495876	0.00171
=	12	=	0.74675	437588	0.00164
=	13	=	0.79123	387252	0.00158
=	14	=	0.82804	343290	0.00153
=	15	=	0.85940	304544	0.00150
=	16	=	0.88054	272698	0.00146
=	17	=	0.89956	244038	0.00144
=	18	=	0.91431	219174	0.00142
=	19	=	0.92532	197602	0.00140
=	20	=	0.93274	178972	0.00139

Sample. H<sub>2</sub>CO

Mass attenuation coefficient = 0.08039 cm<sup>2</sup>/g

Abundance = 0.11% [10]

No. of photon = 10<sup>6</sup>

E<sub>γ</sub> = 0.662 MeV

Detector radius = R<sub>d</sub> = 15 cm

**Table 4-** Shows the calculated density for H<sub>2</sub>CO molecule in C/2009 P1 Garrard Comet.

d <sub>1</sub> (cm)	d <sub>2</sub> (cm)	Real density (g/cm <sup>3</sup> )	Calculated density (g/cm <sup>3</sup> )	No.of incident photon on detector	Error in density (g/cm <sup>3</sup> )
5	11	0.81500	0.78663	498772	0.00196
=	12	=	0.84936	440714	0.00187
=	13	=	0.89898	390826	0.00181
=	14	=	0.94155	346568	0.00175
=	15	=	0.97653	308034	0.00171
=	16	=	1.00032	276194	0.00167
=	17	=	1.02200	247414	0.00164
=	18	=	1.03919	222300	0.00162
=	19	=	1.05162	200638	0.00160
=	20	=	1.05954	182040	0.00158

Sample. HCN

Mass attenuation coefficient = 0.07876 cm<sup>2</sup>/g

Abundance = 0.24% [10]

No. of photon = 10<sup>6</sup>

E<sub>γ</sub> = 0.662 MeV

Detector radius = R<sub>d</sub> = 15 cm

**Table 5-** Shows the calculated density for HCN molecule in C/2009 P1Garradd Comet.

d <sub>1</sub> (cm)	d <sub>2</sub> (cm)	Real density (g/cm <sup>3</sup> )	Calculated density (g/cm <sup>3</sup> )	No.of incident photon on detector	Error in density (g/cm <sup>3</sup> )
5	11	0.69700	0.80760	496746	0.00200
=	12	=	0.87221	438524	0.00192
=	13	=	0.92369	388388	0.00185
=	14	=	0.96726	344198	0.00179
=	15	=	1.00370	305512	0.00175
=	16	=	1.02824	273692	0.00171
=	17	=	1.05027	245066	0.00168
=	18	=	1.06772	220096	0.00166
=	19	=	1.08056	198494	0.00164
=	20	=	1.08896	179904	0.00163

Sample. CH<sub>3</sub>OH

Mass attenuation coefficient = 0.08392 cm<sup>2</sup>/g

Abundance = 2.1% [10]

No. of photon = 10<sup>6</sup>

E<sub>γ</sub> = 0.662 MeV

Detector radius = R<sub>d</sub> = 15 cm

**Table 6-** Shows the calculated density for CH<sub>3</sub>OH molecule in C/2009 P1Garradd Comet.

d <sub>1</sub> (cm)	d <sub>2</sub> (cm)	Real density (g/cm <sup>3</sup> )	Calculated density (g/cm <sup>3</sup> )	No.of incident photon on detector	Error in density (g/cm <sup>3</sup> )
5	11	0.79100	0.75312	498966	0.00188
=	12	=	0.81333	440846	0.00180
=	13	=	0.86065	391044	0.00173
=	14	=	0.90154	346732	0.00168
=	15	=	0.93495	308230	0.00164
=	16	=	0.95791	276316	0.00160
=	17	=	0.97845	247612	0.00157
=	18	=	0.99496	222472	0.00155
=	19	=	1.00680	200826	0.00153
=	20	=	1.01429	182248	0.00152

Sample. H<sub>2</sub>O

Mass attenuation coefficient = 0.08510 cm<sup>2</sup>/g

Abundance = 100% [10]

No. of photon = 10<sup>6</sup>

E<sub>γ</sub> = 0.662 MeV

Detector radius = R<sub>d</sub> = 15 cm

**Table 7-** Shows the calculated density for H<sub>2</sub>O molecule in C/2009 P1Garradd Comet.

d <sub>1</sub> (cm)	d <sub>2</sub> (cm)	Real density (g/cm <sup>3</sup> )	Calculated density (g/cm <sup>3</sup> )	No.of incident photon on detector	Error in density (g/cm <sup>3</sup> )
5	11	0.91700	0.73812	501096	0.00185
=	12	=	0.79647	443370	0.00177
=	13	=	0.84277	393624	0.00170
=	14	=	0.88217	349580	0.00165
=	15	=	0.91481	311064	0.00161
=	16	=	0.93787	278872	0.00157
=	17	=	0.95834	249966	0.00155
=	18	=	0.97420	224860	0.00152
=	19	=	0.98505	203370	0.00150
=	20	=	0.99255	184644	0.00149

Sample. CH<sub>4</sub>

Mass attenuation coefficient = 0.08845 cm<sup>2</sup>/g

Abundance = 0.8% - 0.9% [10]

No. of photon = 10<sup>6</sup>

E<sub>γ</sub> = 0.662 MeV

Detector radius = R<sub>d</sub> = 15 cm

**Table 8-** Shows the calculated density for CH<sub>4</sub> molecule in C/2009 P1 Garradd Comet.

d <sub>1</sub> (cm)	d <sub>2</sub> (cm)	Real density (g/cm <sup>3</sup> )	Calculated density (g/cm <sup>3</sup> )	No.of incident photon on detector	Error in density (g/cm <sup>3</sup> )
5	11	0.44200	0.72588	493492	0.00179
=	12	=	0.78431	434974	0.00171
=	13	=	0.83052	384824	0.00165
=	14	=	0.86955	340696	0.00160
=	15	=	0.90243	302010	0.00156
=	16	=	0.92428	270348	0.00153
=	17	=	0.94485	241538	0.00151
=	18	=	0.96025	216792	0.00149
=	19	=	0.97213	195204	0.00147
=	20	=	0.98024	176568	0.00146

Sample. NH<sub>3</sub>

Mass attenuation coefficient = 0.08970 cm<sup>2</sup>/g

Abundance = 0.5% [10]

No. of photon = 10<sup>6</sup>

E<sub>γ</sub> = 0.662 MeV

Detector radius = R<sub>d</sub> = 15 cm

**Table 9-** Shows the calculated density for NH<sub>3</sub> molecule in C/2009 P1 Garradd Comet.

d <sub>1</sub> (cm)	d <sub>2</sub> (cm)	Real density (g/cm <sup>3</sup> )	Calculated density (g/cm <sup>3</sup> )	No.of incident photon on detector	Error in density (g/cm <sup>3</sup> )
5	11	0.81700	0.70196	500264	0.00176
=	12	=	0.75797	442252	0.00168
=	13	=	0.80205	392478	0.00162
=	14	=	0.83966	348384	0.00157
=	15	=	0.87061	309930	0.00153
=	16	=	0.89236	277838	0.00149
=	17	=	0.91181	248972	0.00147
=	18	=	0.92674	223954	0.00145
=	19	=	0.93759	202314	0.00143
=	20	=	0.94458	183678	0.00142

**Table 10-** Shows the calculated density for Nine molecules in C/2009 P1 Garradd Comet.

No.	E <sub>γ</sub>	d <sub>1</sub>	d <sub>2</sub>	ρ <sub>Real</sub>	ρ <sub>Cal</sub>	Δρ	R <sub>c</sub>	R <sub>d</sub>
1	0.662	5	13	0.815	0.812	0.00182	H <sub>2</sub> CO	15
2	=	=	18	0.917	0.910	0.00146	H <sub>2</sub> O	=
3	=	=	=	0.789	0.791	0.00206	CO	10
4	=	=	=	0.724	0.735	0.00191	C <sub>2</sub> H <sub>2</sub>	10
5	0.2	=	20	0.546	0.540	0.00083	C <sub>2</sub> H <sub>6</sub>	15
6	=	=	14	0.442	0.451	0.00089	CH <sub>4</sub>	15
7	0.3	=	17	0.697	0.696	0.0016	HCN	15
8	0.5	=	17	0.791	0.786	0.00131	CH <sub>3</sub> OH	15
9	0.6	=	17	0.817	0.814	0.00136	NH <sub>3</sub>	15
10	0.7	=	13	0.815	0.815	0.00175	H <sub>2</sub> CO	15
11	0.9	=	14	0.917	0.927	0.00183	H <sub>2</sub> O	15

**Conclusions:**

1. The geometry system can be used to calculate the efficiency for different detectors.
2. Using Monte Carlo method enable us to choose a wider range of energies.
3. The simulation results are very near from the real values as shown in Table-10. This proves the accuracy of the program and geometry.
4. From the results, that the increases of photon gamma energy that reaches to the detector causes decreasing in the number of incident photon on detector (Count rate). Because the escaping probability of the photon from the sample will be increase.
5. The sample thickness is inversely proportional with the variation of number of incident photon on detector (Count rate).
6. In general, the best values for densities have been obtained from Monte Carlo simulation method at energies 0.662 MeV and 0.7 MeV. This means that Compton scattering is very active in these energies.

**Reference:**

1. Sherrod, P.C. and Koed, T.L. **2012**. A Complete Manual of Amateur Astronomy: *Tools and Techniques for Astronomical Observations*. Courier Corporation, pp: 65-67.
2. Al Bermani, M. J. F., Alhamed, S.A., Khalaf, S. Z, Ali, H. Sh and Selman, A. A. **2009**. Three dimensional explicit model for cometary tail ions interactions with solar wind. *Journal of Al-Nahrain University*, 12(2), pp: 68-75.
3. Brandt, J.C. and Chapman, R.D. **2004**. *Introduction to Comets*. Cambridge University Press, pp:10- 15.
4. Lippi, V. M. **2010**. The Composition of Cometary ices as inferred from measured production rates of Volatiles. Ph.D. Thesis. University of Carolo-Wilhelmina, Italian.
5. Faure, G. and Teresa, M. M. **2007**. *Introduction to Planetary Science*. Springer Science and Business Media, pp: 424-430.
6. Buroham, R. **2000**. *Great Comets*. Cambridge University Press, pp: 34-36.
7. Meierhenrich, U. **2015**. *Comets and Their Origin*. John Wiley and Sons, pp:17-21.
8. Zell- Ravenheart, O. and Faculty of the Grey School of Wizardry. **2006**. *Companion for the Apprentice Wizard*. Career Press. pp:188-190.
9. Hubbell J. H. **1982**. Photon mass attenuation and energy- absorption coefficients. *The International Journal of Applied Radiation and Isotopes*, 33(11), pp:1269- 1290.
10. DiSanti, M. A., Villanueva, G. L., Paganini, L., Bonev, B. P., Keane, J. V., Meech, K. J. and Mumma, M. J. **2014**. Pre- and post-perihelion observations of C/2009 P1 (Garradd): Evidence for an oxygen-rich heritage? *Elsevier*, 228, pp:167- 180.